

Pyruvate Ferredoxin Oxidoreductase and Its Radical Intermediate[†]

Stephen W. Ragsdale

Department of Biochemistry, Beadle Center, 19th and Vine Streets, University of Nebraska, Lincoln, Nebraska 68588-0664

Received August 8, 2002

Contents

I. Introduction	2333
A. Prospectus	2333
B. Metabolic Role of PFOR	2335
II. The Catalytic Machines: The Protein and the Cofactor TPP	2336
A. Structure of PFOR	2336
B. What Is so Special about TPP? Intramolecular Interactions in the Cofactor	2337
C. Intermolecular Interactions between TPP and PFOR	2338
III. Intermediates in the PFOR Reaction	2338
A. Early Steps in the PFOR Reaction: Commonality among TPP Enzymes	2338
B. The Fates of HE–TPP: Convergent and Divergent Mechanisms	2340
C. PFOR and Its Radical Mechanism	2340
D. Electronic Structure of the Radical Intermediate	2340
E. Reactivity of the HE–TPP Radical Intermediate: Chemical Coupling, Biradicals, and Wires	2342
F. Reaction of Fully Reduced PFOR with Electron Acceptors	2345
IV. Perspective and Prospective	2345
V. Abbreviations	2345
VI. References	2345



Stephen W. Ragsdale was born in Rome, GA, in 1952. He received his BS and PhD degrees in Biochemistry from the University of Georgia, where he began research in Microbial Biochemistry and Enzymology with Dr. Lars Ljungdahl. After graduating in 1983, he was an NIH Postdoctoral Associate with Harland G. Wood at Case Western Reserve University in Cleveland, OH. In 1987, he joined the Chemistry faculty at the University of Wisconsin–Milwaukee, where he was honored as a Shaw Scholar and continued studying microbial acetate biosynthesis, including nickel, iron–sulfur, and vitamin B₁₂ containing enzymes. After joining the Biochemistry Department at the University of Nebraska as Associate Professor in 1991, he became full Professor in 1996. He has published over 100 papers spanning the research areas of microbial biochemistry, environmental biochemistry, metallobiochemistry, and enzymology. Recent research highlights include discovering (with C. Drennan) a novel metallocenter containing nickel, copper, and iron–sulfur; uncovering (with M. Maroney and D. Bocian) a plausible activation mechanism of the key enzyme in methanogenesis; and finding a new role for Coenzyme A in regulating electron transfer in pyruvate:ferredoxin oxidoreductase, the topic of this review. He has served on various committees in the American Chemical Society, including Treasurer of the Biological Chemistry Division, and in the American Society of Microbiology, where he recently served as Chair of the Microbial Physiology Division. Other activities include Editorial Board memberships on *Journal of Biological Chemistry* (1997–2002, 2003–2008), *Journal of Bacteriology* (1996–2004), *Archives of Microbiology* (2003–2006), *BioFactors* (1987–present), and *Archives of Biochemistry and Biophysics* (1999–2002); several Study Sections at NIH; and grant review panels for Department of Energy and NSF. Of the 16 graduate students and 17 postdoctoral associates that he has advised over the past 15 years, two are now faculty members in Academia, and others are in industry.

I. Introduction

A. Prospectus

This article reviews an enzyme that has the ability to perform the thiamine pyrophosphate (TPP)-dependent oxidative decarboxylation of pyruvate to form acetyl-CoA and CO₂. Because the pyruvate:ferredoxin oxidoreductase (PFOR) reaction is reversible, the enzyme has also been called pyruvate synthase. Two key steps in the mechanism are the generation and decay of a substrate-derived hydroxyethyl–TPP radical (HE–TPP) intermediate. In this review, “HE–TPP” will refer to hydroxyethyl–TPP, 2 α -hydroxyethylidene–TPP, as well as the radical, so the modifier “anion” or “radical” will usually be added to clarify which form of the intermediate is

being discussed. Because the emphasis of this *Chemical Reviews* volume is on radicals in biology, the properties of the radical will be a major focus. First, the early steps leading to the formation of the two key intermediates, the ylide and the anionic 2 α -hydroxyethylidene–TPP, which are common to a variety of TPP-dependent enzymes, will be discussed. This section will focus on the factors that lead to a 10¹²-fold rate enhancement for deprotonation of the C2-thiazolium proton and the C2 α proton of

[†] Research on PFOR has been supported by a grant from the National Institutes of Health (GM39451) to S.W.R.
* Phone: 402-472-2943. Fax: 402-472-7842. E-mail: sragdale1@unl.edu.

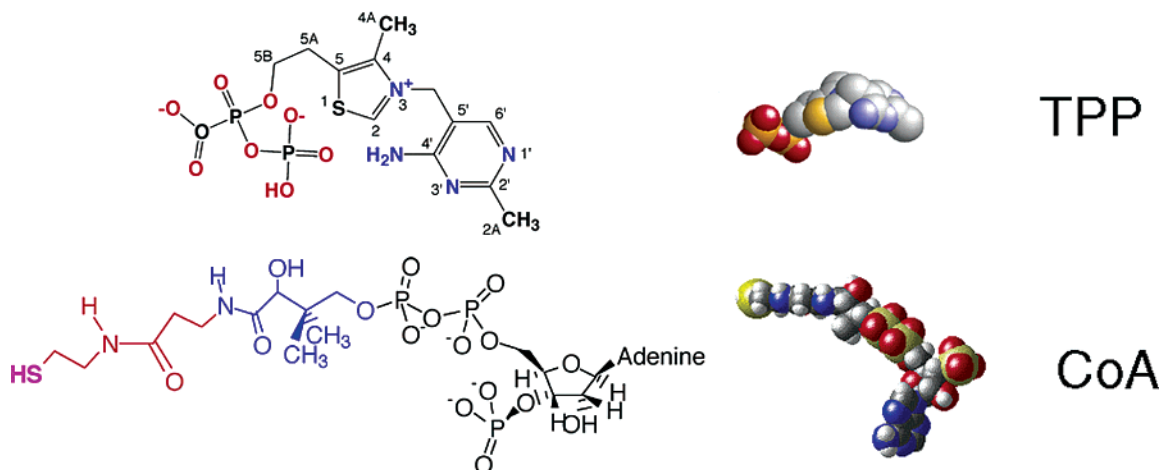


Figure 1. PFOR Cofactors.

HE–TPP. Unlike most TPP-dependent enzymes, in PFOR, the HE–TPP intermediate undergoes a one-electron oxidation to form the hydroxyethyl–TPP radical intermediate. A provocative hypothesis, based on the crystal structure of the radical, of an acetyl radical with a tenuous bond to a thiazolium ring that has lost its aromaticity will be discussed. The stability of this radical is profoundly affected by binding of CoA. How CoA causes a 100 000-fold enhancement of the rate of radical decay will be described. Finally, how the low-potential electrons from pyruvate decarboxylation are transferred to external acceptors will be discussed.

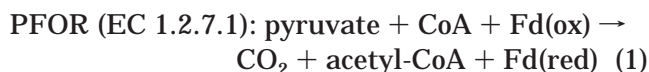
Since pyruvate is a central metabolite, the various biochemical anabolic and catabolic reactions involving pyruvate have been studied for many decades. In writing a review of a system with such a long history, I am reminded of a precept I saw on the wall of Bill Antholine's office at the National Biomedical ESR center in Milwaukee:

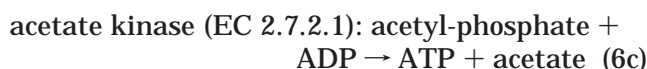
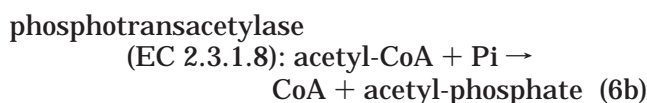
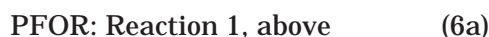
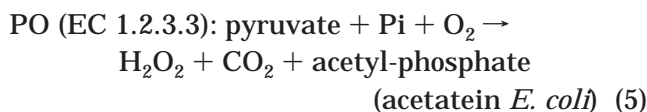
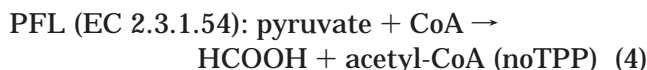
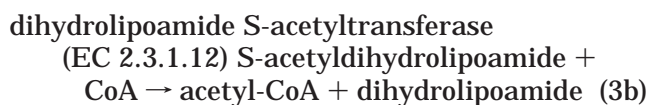
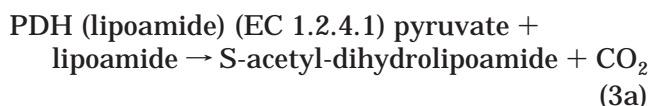
"We have not succeeded in answering all our problems. The answers we have found only serve to raise a whole set of new questions. In some ways we feel we are as confused as ever, but we believe we are confused on a higher level and about more important things."

This article focuses on the question: how are pyruvate and related α -keto acids, like α -ketoglutarate, oxidized? This question has been asked in different ways and at different levels of sophistication for at least seven decades. Pursuit of the answer has led to the discovery of cofactors, the elucidation of pathways, the development of concepts in bioenergetics, and the elucidation of novel reaction intermediates. Fritz Lipmann asked that question in 1937 and, using extracts of *Lactobacillus*, isolated acetyl phosphate, one of the first examples of "squiggle phosphate".¹ Further experiments led to the isolation and identification of coenzyme A (CoA) from pigeon liver extracts as an acetyl carrier forming "active acetate" or acetyl-CoA, which was found to be involved in many biochemical reactions.² It was Fyodor Lynen who demonstrated the thioester linkage in acetyl-CoA. In elucidating the structure, Lipmann and co-workers found that CoA contains the vitamin, pantothenic acid. For the discovery and elucidation of the roles of CoA, Lipmann was awarded the 1953

Nobel prize (with Hans Krebs). Peters and Ochoa demonstrated that pyruvate oxidation requires thiamin diphosphate, which had been isolated earlier^{3,4} (Figure 1). Thiamin, vitamin B1, had recently been identified as the factor whose absence causes beriberi. In 1937, Lohmann and Schuster described the structure of this thermostable organic cofactor, "cocarboxylase", as "aneurinpyrophosphat" or thiamin pyrophosphate (thiamin diphosphate).⁵ In the 1950s O'Kane and Gunsalus at Cornell were trying to identify a "pyruvate oxidation factor" that was necessary for oxidation of pyruvate to acetate and carbon dioxide by *Streptococcus faecalis*. This factor was eventually purified 300 000-fold by Reed and Gunsalus from 10 tons of liver⁶ and characterized as 6,8-dithiooctanoic acid (lipoic acid).⁷ Studies of pyruvate oxidation also led to the discovery of ferredoxin.^{8,9}

We now know of at least five possible pathways of pyruvate oxidation (eqs 1–5). In PFOR (eq 1), a low-potential reductant, ferredoxin or flavodoxin, is reduced by one electron, leaving a radical intermediate that can drive other low-potential reactions (H_2 formation, hydrogenase; N_2 fixation, nitrogenase; and CO_2 reduction to CO (CO dehydrogenase) or formate (formate dehydrogenase)). PFOR is also the target for metronidazole, which is a commonly used pharmaceutical, for example, for *Helicobacter pylori* eradication regimes to control ulcers.¹⁰ Although PO (reaction 5) has often been considered to be a nonessential, perhaps even wasteful, reaction of uncertain function, *Escherichia coli* PO null mutants have a significantly reduced growth rate, suggesting an important role for PO during aerobic growth.¹¹ PDH (reaction 3) in aerobes is used to deplete excess reducing equivalents and to generate NADH, which donates electrons to the mitochondrial electron transfer chain for oxidative phosphorylation. PDC (reaction 2) is the key enzyme in ethanol fermentation reactions; however, PDC is absent in animals and relatively rare in bacteria:





Many organisms such as *E. coli* are interesting because they contain most of the above enzymes (although *E. coli* does not have a PDC) and differentially regulate their expression depending on growth conditions. Under aerobic conditions, PDH, which generates NADH for oxidative phosphorylation, and PO are expressed,^{12,13} while under anaerobic conditions, PFOR and PFL (reaction 4) are expressed.¹⁴

This review focuses on PFOR, which is a component of reactions that were collectively called the phosphoroclastic reaction (eqs 6a–6c). In 1953, using extracts from *Clostridium butyricum*, Wolfe and O'Kane, demonstrated that the phosphoroclastic reaction required thiamin pyrophosphate (TPP) and CoA, like the liver extracts; however, it also needed

ferrous ion and, surprisingly, did not require lipoic acid.¹⁵ By 1962, ferredoxin was found to be the electron acceptor for the phosphoroclastic reaction.^{8,9} In the 1940–1960s, only impure preparations from animal tissues and microbes were available, not isolated enzymes. It took many years before a PFOR was purified to near homogeneity. This was accomplished by Uyeda and Rabinowitz,¹⁶ who published four back-to-back papers describing the cofactor (FeS, thiamine) content and the kinetic properties of the PFOR from *Clostridium aciduriaci*.^{16–19}

B. Metabolic Role of PFOR

PFOR is an ancient molecule that existed before divergence of the archaea and eukaryotes (Figure 2). All members of the Archaea kingdom appear to contain PFOR; it is widely distributed among bacteria, and anaerobic protozoa like *Giardia* also have PFOR.²⁰

PFOR is involved in catabolic as well as anabolic pathways. The oxidation of pyruvate by PFOR generates low-potential electrons ($E_0' = -540$ mV) that reduce ferredoxin or flavodoxin.^{10,21–25} In anaerobic bacteria, PFOR is generally part of the phosphoroclastic system, which allows the generation of ATP from acetyl-CoA through substrate-level phosphorylation (reactions 6a–c, above). Sulfate reducing bacteria couple the oxidation of pyruvate to the reduction of SO_4 or protons, forming H_2S or H_2 , respectively, during the metabolism of lactate, fumarate, malate, or alanine to acetate.^{26,27} *Pyrococcus* and *Thermococcus* appear to couple PFOR/ferredoxin to the reduction of elemental sulfur to sulfide.²⁸ In nitrogen-fixing organisms, PFOR (NifJ) provides low-potential electrons to dinitrogenase reductase,²⁴ the electron donor for nitrogenase. In acetogenic bacteria, PFOR links the Embden–Meyerhof pathway to the Wood–Ljungdahl pathway of acetyl-CoA synthesis.^{29,30} In *Helicobacter pylori*, which grows under microaerophilic conditions, PFOR (PorCDAB) is linked to an NADP:flavodoxin oxidoreductase through flavodoxin (fldA).^{10,31} Although the metabolic significance is unknown, the *Pyrococcus* PFOR apparently can form acetaldehyde from pyruvate.³² PFOR also has the

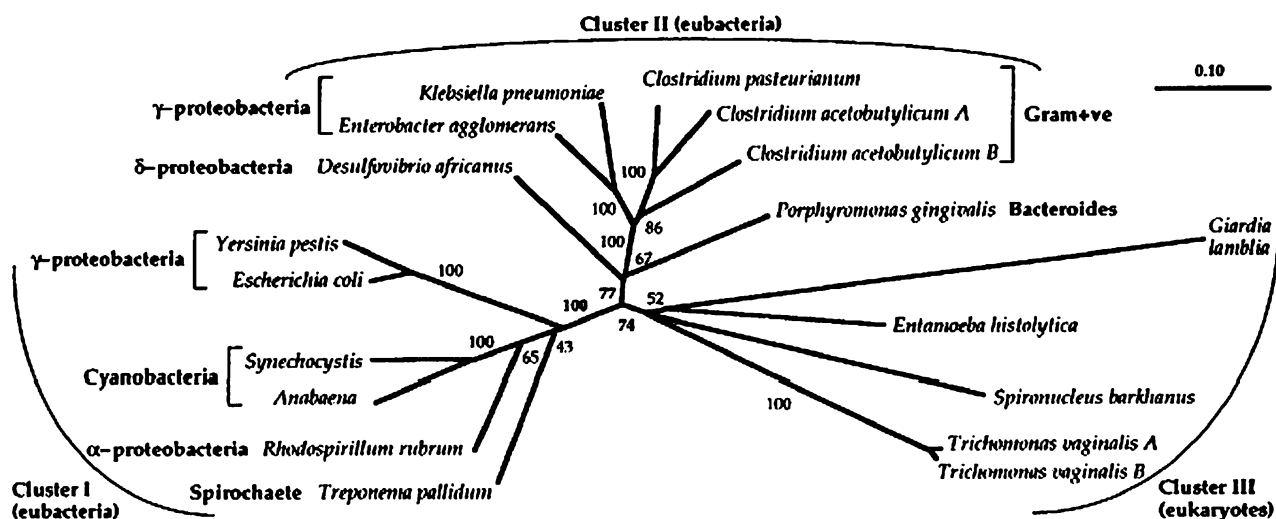


Figure 2. Evolution of PFOR. From ref 20.

ability to reduce protons to H_2 .³³ H_2 production is extremely slow and occurs only when electron acceptors are not available to oxidize PFOR, indicating that this is not metabolically significant source of H_2 ; however, it has been proposed that this reaction has evolved to “defuse” the radicals (reduced FeS clusters and radical intermediate) that are formed during the catalytic cycle when oxidized redox mediators are present in limiting amounts.³³

The oxidation of pyruvate by PFOR is also an important step in the anaerobic metabolism of glucose by amitochondriate eukaryotes, some of which contain hydrogenosomes.^{20,34} These organisms include the gut protozoan parasite *Giardia* and the reproductive tract parasite, *Trichomonas vaginalis*. The importance of PFOR in their metabolism renders them susceptible to nitroimidazole drugs, such as metronidazole and tinidazole, which are common treatments for these parasites.³⁵ The mechanism of action is generation of a nitro radical that can undergo further reactions to form nitroso and hydroxylamine radicals (Figure 3). In *Helicobacter pylori*,

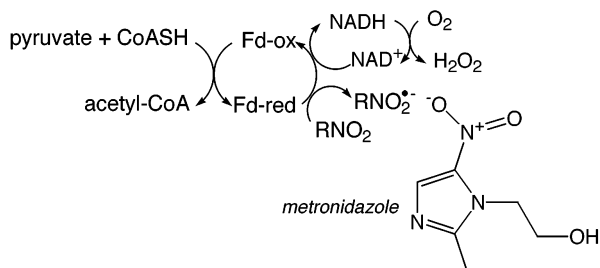


Figure 3. The mechanism of PFOR-targeted antiparasite drugs.

resistance to metronidazole involves repression of PFOR (Por) and constitutive expression of isocitrate lyase.³⁶

Three α -ketoacid oxidoreductases with significant sequence homology to PFOR have been characterized from the hyperthermophilic archaeon *Pyrococcus furiosus*.²⁸ These enzymes, α -ketoglutarate:isovalerate and indolepyruvate:ferredoxin oxidoreductase, function in the oxidation of the amino acids glutamate, leucine, and tryptophan. All these enzymes are dimers of heterotetramers with subunit M_r of 43, 35, 23, and 12 kDa. The overall molecular mass of each of these enzymes is 220 kDa, which is similar to that of the homodimeric enzyme from bacteria. Thus, the minimum molecular mass for a single catalytic component is \sim 120 kDa. Like PFOR, the α -ketoacid oxidoreductases contain FeS clusters and TPP.

In anaerobes, the reverse (anabolic) reaction of pyruvate formation is feasible, provided that a sufficiently low-potential electron donor is available. This is not possible with the PDH complex because its requisite electron donor, NADH, is much too weak an electron source to reduce acetyl-CoA (the NAD/NADH half reaction is 200 mV more positive than the acetyl-CoA/pyruvate couple). The reverse reaction, carboxylation of acetyl-CoA, is an important reaction because it serves to assimilate CO_2 into cell carbon. Anaerobes have designed a variety of systems to accomplish this task. In some anaerobes, CO (and CO dehydrogenase) can be used as an electron source

(the CO_2/CO half reaction is \sim -520 mV) for the back reaction.³⁰ In methanogens, pyruvate formation appears to require reverse electron-transfer involving coupling of H_2 oxidation by the membrane-associated *Ech* hydrogenase to the membrane.³⁷ For anaerobes such as methanogens and acetogens that fix CO_2 by the Wood–Ljungdahl pathway,^{38,39} PFOR (pyruvate synthase) links the Wood–Ljungdahl pathway to the incomplete reductive tricarboxylic acid cycle, which generates biosynthetic intermediates. PFORs have been isolated from the acetogenic bacterium *Moorella thermoacetica* (f. *Clostridium thermoaceticum*)^{29,30} and from the methanogenic archaea, *Methanosarcina barkeri*⁴⁰ and *Methanobacterium thermoautotrophicum*.⁴¹ These enzymes must function in anabolic reactions, since methanogens cannot grow on substrates with a more complex structure than acetate. The *M. barkeri* enzyme was shown to catalyze the oxidative decarboxylation of pyruvate to acetyl-CoA and the reductive carboxylation of acetyl-CoA with ferredoxin as an electron carrier.⁴² The sequences of the methanogenic enzymes^{41,42} are closely related to those of the PFORs from *Pyrococcus furiosus* and *Thermotoga maritima*, which function in a catabolic direction.⁴³ Thus, these combined studies indicate that the same enzyme (PFOR) functions physiologically in either direction. This conclusion is supported by the finding that under some conditions, methanogens can grow, albeit poorly, on pyruvate.^{44,45} Yoon et al. have also studied the pyruvate synthase reaction of the PFOR from *Chloribium tepidum*,⁴⁶ which, like the methanogens, links to the incomplete TCA cycle to convert oxaloacetate (derived from pyruvate by the action of pyruvate carboxylase or the linked activities of phosphoenolpyruvate (PEP) synthetase and PEP carboxylase) into malate, fumarate, succinate, succinyl-CoA, and α -ketoglutarate.³⁸

II. The Catalytic Machines: The Protein and the Cofactor TPP

A. Structure of PFOR

The overall quaternary structure of PFOR is quite variable. Most bacterial PFORs are homodimeric (A2, Figure 4); yet the *Halobacterium* enzyme is het-

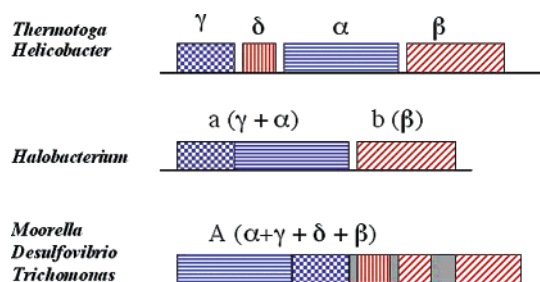


Figure 4. Domain arrangement in PFORs. Modified from Kletzen and Adams, 1996, with permission from ASM Journals Department.²³

erodimeric (ab), apparently having lost a domain. A heterotetrameric enzyme, like the archaeal PFORs, has been proposed to be the common ancestor^{23,47} that underwent gene rearrangement and fusion to account for the hetero- and homodimeric enzymes. The δ

subunit (or domain for the bacterial PFORs), which was lost in the Halobacterium enzyme, contains the cysteine residues to coordinate two [4Fe–4S] clusters (the medial and distal clusters, see below). The β domain coordinates the proximal [Fe₄S₄]^{2+/1+} cluster and contains a conserved TPP binding site.

The 2.3 Å resolution crystal structure of the *Desulfovibrio africanus* PFOR (Figure 5) indicates that

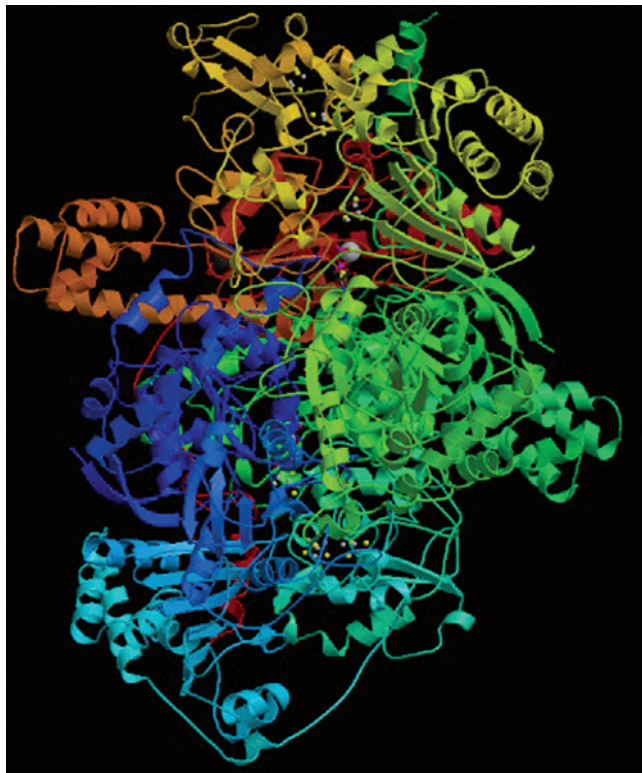


Figure 5. Overall PFOR structure. From PDB code 1KEK.

there are seven structural domains. TPP and a proximal [Fe₄S₄]^{2+/1+} cluster (designated cluster A) are buried within the protein and that two additional [Fe₄S₄]^{2+/1+} clusters (cluster B and cluster C) lead toward the surface, where interactions with a redox partner such as ferredoxin can occur.⁴⁸ Each of the three clusters is separated by ~13 Å (center-to-center). The *D. africanus* enzyme, unlike most PFORs, is oxygen-stable, and its three clusters exhibit midpoint redox potentials of –540, –515, and –390 mV, although it was not possible to assign these midpoint potentials to specific clusters.⁴⁹ Structural domain VI, which is proposed to derive from the ancestral β subunit, is part of the TPP binding fold, which includes domains I and III. This fold is conserved in transketolase, PO, and PDC.⁴⁸ Domain VI (and the β subunit) also contains conserved cysteine residues 812, 815, 840, and 1071, which ligate the proximal [4Fe–4S] cluster (cluster A). Domain V, which derives from the ancestral δ subunit, contains that eight-Fe ferredoxin-like domain that includes the eight cysteine residues required for binding the medial and distal [4Fe–4S] clusters. Domain VII is lacking in many PFORs (it is not shown in Figure 4) and, since the *D. africanus* PFOR is unusually insensitive to oxygen, has been proposed to stabilize the enzyme against oxygen damage.

B. What Is so Special about TPP? Intramolecular Interactions in the Cofactor

Understanding thiazolium chemistry is the key to understanding the TPP-dependent oxidative decarboxylation of pyruvate and other α -keto acids (for a review, see Jordan⁵⁰). When the structure of TPP was determined,⁵ attention focused on the 4'-amino group of the pyrimidine ring as the key catalytic component of TPP because primary amines had been found to stimulate the decarboxylation of α -ketoacids. A paradigm shift occurred when Ron Breslow discovered that the C-2 proton of the thiazolium ring undergoes exchange in D₂O.^{51,52} This result is remarkable because the C2–H of free TPP in water has a pK_a of 17–19!⁵³ The pK_a of the C2(α) for hydroxybenzylthiamine-PP is 15.4 in water.^{1,54,55}

Deprotonation of the C2–H generates a highly nucleophilic thiazolium anion, in which the negative charge is delocalized through the thiazolium ring, including the sulfur d-electrons. Although the thiazolium is highly reactive, the coenzyme appears to be predominantly in the unreactive, protonated state, with an undissociated proton at C-2, in solution as well as when bound to the enzyme;⁵⁶ however, Jordan points out that various factors related to the nuclear relaxation of the C2 carbon, uncertainties in the chemical shift, and the huge mass of the enzyme make this a difficult experiment to interpret.⁵⁷ When hydroxybenzyl–TPP (resembles the HE–TPP intermediate) binds to PDC, the C2 α proton is fully dissociated at pH 6.0, indicating that the enzyme decreases the pK_a of C2–H of the bound HE–TPP analogue by >9 pK_a units.⁵⁷ The same factors responsible for lowering the pK_a of this analogue could also conspire to lower the pK_a of the C2 of TPP to generate the thiazolium anion, however, the rate of deprotonation is faster than the overall rate of the reaction, so thermodynamic stabilization of the thiazolium anion may not be required for catalysis.

Enhancement of the rate of deprotonation of C2 plays an important role in TPP-dependent enzymes. For example, if 1% of the TPP is in the ylide form, then that 1% of the enzyme is catalytically active. However, if deprotonation of C2–H occurs >100-fold faster than the *k*_{cat} for the reaction, this step will not be rate determining for the overall reaction. So far, the pK_a for the C2–H in enzyme-bound TPP has not been measured; however, it is estimated that the dissociation rate must be enhanced by at least 10⁴-fold to overcome the unfavorable pK_a (assuming that the C2–H is predominantly in the protonated state, see above). When pyruvate decarboxylase is incubated with TPP in the presence of pyruvamide, an activator whose binding site is far from that of TPP, the rate of the H/D exchange for the C2–H of TPP is greater than 600 s^{–1}, which is at least 10⁶-fold faster than that in free TPP.⁵⁸ A similar enhancement of the rate of deprotonation of the thiazolium C2–H is observed in pyruvate dehydrogenase, pyruvate oxidase, and transketolase, indicating a common mechanism. Is deprotonation stepwise or concerted with substrate binding? Even in the absence of substrates, a high H/D exchange rate is observed,⁵⁸ indicating that this is a stepwise mechanism.

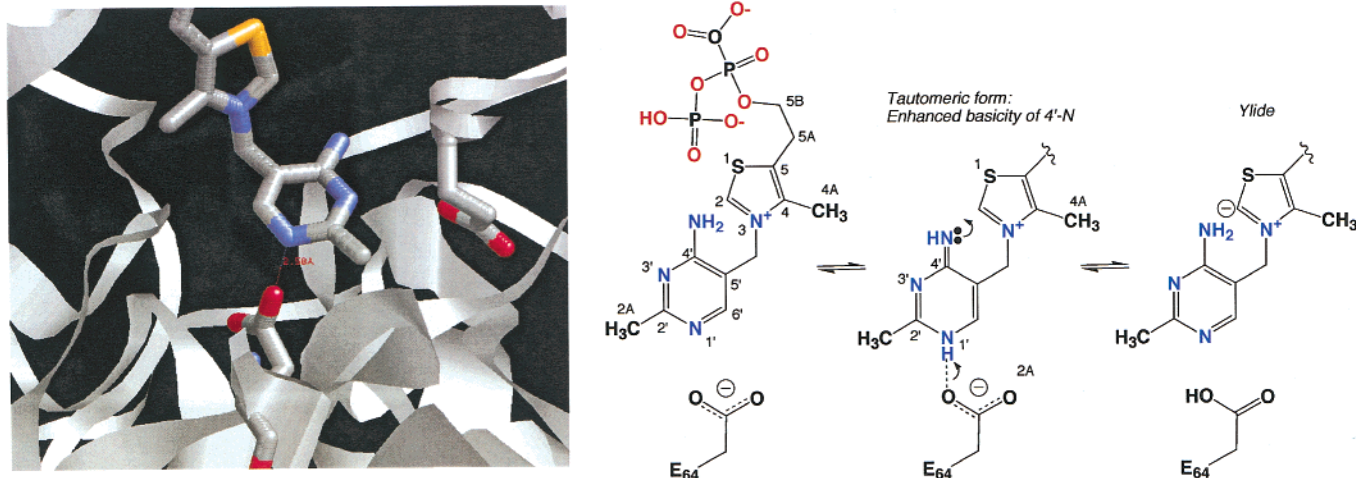


Figure 6. The mechanism of generation of the active thiazolium catalyst. (a) Deprotonation of TPP. E64 is shown in the left corner. From PDB code 1BOP. (b) Generation of the ylide intermediate

Given the above discussion, it is of considerable importance to understand how the TPP-dependent enzymes enhance the thermodynamics and kinetics of dissociation of the C-2 thiazolium proton. How is this deprotonation accomplished? Intermolecular and intramolecular interactions have been identified that play a role. Associations between the cofactor and the enzyme will be classed as intermolecular, while interactions between functional groups on the cofactor will be called intramolecular. In all the above-mentioned enzymes, intermolecular interactions between a functionally conserved acidic group and the N1' atom of the pyrimidine ring (Figure 6a locates E64 in PFOR) drive the thiazolium into a tautomeric form, exhibiting increased basicity for the N4' nitrogen atom (Figure 6b). Intramolecular interactions between the N4' pyrimidine and C2 of the thiazolium promote deprotonation of C2, generating the active ylide. In the *D. africanus* PFOR, the distance between E64 and N1' is 2.6 Å. Mutagenesis studies support the requirement for this group; for example, in transketolase, mutation of the corresponding residue (E418) to alanine decreases the H/D exchange rate 200-fold.⁵⁸ Similarly, in pyruvate decarboxylase, mutation of E51 to glutamine decreases the rate of H/D exchange 300-fold.⁵⁸ Thus, a major part of the rate enhancement results from intramolecular interactions between the N1' pyrimidine and the C2-H.

C. Intermolecular Interactions between TPP and PFOR

Besides the specific interaction between E64 and the N1' pyrimidine, the overall environment of the TPP binding site in PDC has a low dielectric constant of 13–15, which is similar to that of *n*-pentanol (water has a value of 80).⁵⁷ It was estimated that the effects of this low dielectric medium can account for ~7 kcal/mol of the ~13 kcal/mol stabilization of the zwitterionic thiazolium and the dissociated HE–TPP anion intermediates. Similar studies should be performed on other TPP-dependent enzymes, especially PFOR.

Presuming that a lowering of the dielectric constant at the active site of PFOR does enhance

catalysis as in PDC, what can account for the other ~6 kcal/mol of stabilization of the dissociated C2 α anion? A large degree of this stabilization is likely to derive from intermolecular interactions between E64 and the N1' pyrimidine. Several other specific interactions are important for binding TPP and could enhance catalysis (Figure 7). The TPP binding fold in PFOR consists of two structurally similar domains as found in transketolase, pyruvate oxidase, and pyruvate decarboxylase.⁵⁹ Mg²⁺ is bound by the pyrophosphate, by a conserved GDG motif, and through interactions with T991 and E817. The pyrophosphate interacts extensively with amino acid residues T965 (amide N), S995 (amide N), E817 (carboxyl O), C840 (amide N), N996 (N), and two water molecules. Conserved residue N996 also forms a hydrogen bond interaction with the thiazolium sulfur of TPP. One of the most important interactions is an aromatic stacking of F869 (which is in the position of I415 in pyruvate decarboxylase) and the thiazolium ring. This interaction promotes formation of the V-conformation between the pyrimidine and thiazolium ring, which is conserved in all the TPP-dependent enzyme so far studied.⁶⁰

The various interactions between the enzyme and TPP that have been described above are thought to be extremely important for catalysis. It is estimated that PDC accelerates the rate of pyruvate decarboxylation by 10¹²-fold relative to TPP in solution.⁶¹ As pointed out by Jordan, the >9 unit suppression of the pK_a of the thiazolium C2 α could account for a 10⁹-fold rate enhancement.⁵⁷

III. Intermediates in the PFOR Reaction

A. Early Steps in the PFOR Reaction: Commonality among TPP Enzymes

After recognizing the importance of the thiazolium in TPP reactions, Breslow proposed a mechanism that has remained at the heart of all subsequent catalytic mechanisms of TPP-dependent decarboxylases (Figure 8).^{51,52} His prediction of a hydroxyethyl adduct with C-2 of the thiazolium, "active acetaldehyde", was confirmed when pyruvate decarboxylase

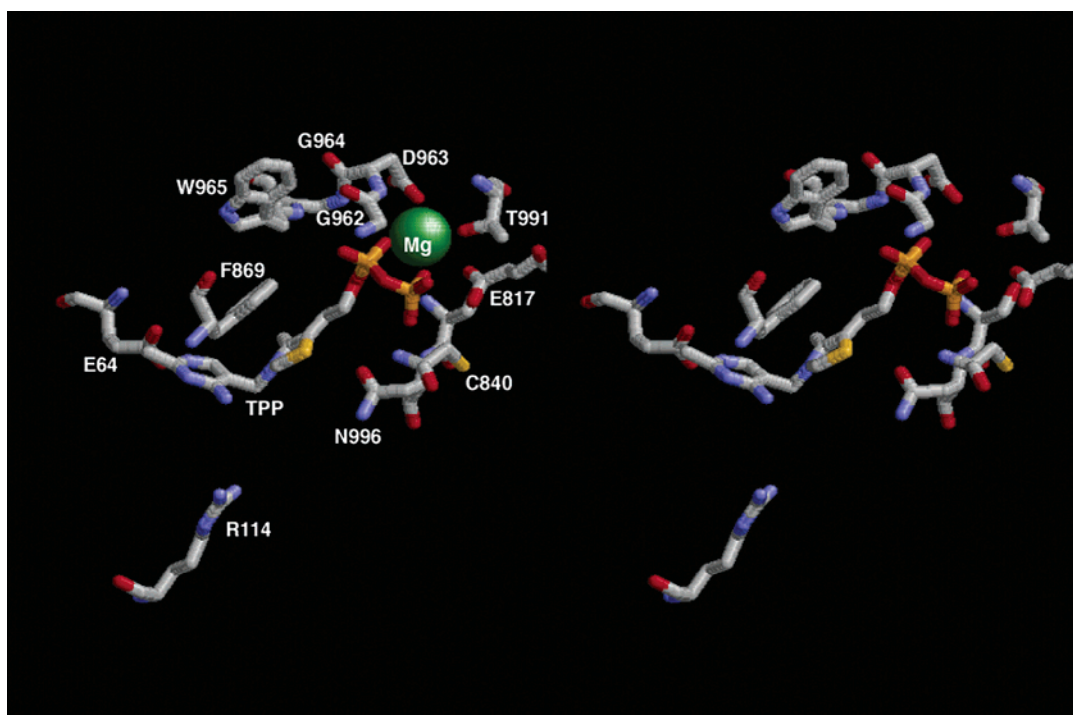


Figure 7. Specific PFOR–TPP interactions at the active site. From PDB code 1KEK.

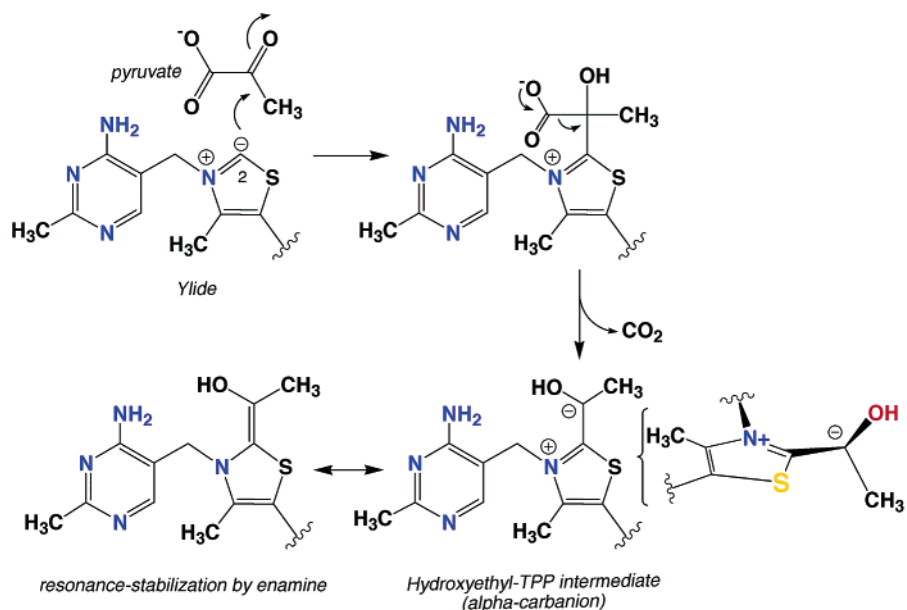


Figure 8. Formation of the HE–TPP intermediate.

was incubated with 2-¹⁴C-labeled pyruvate and the appropriately labeled 2-([1-¹⁴C]-1-Hydroxyethyl)TPP intermediate was identified.⁶² The pyruvate–PFOR adduct and the HE–TPP radical intermediate (or, as proposed, the acetyl–TPP radical) have also been identified in the crystal structures of the *D. africanus* PFOR (Figure 9).⁶³

There are two high-energy intermediates in this reaction pathway. The first is the ylide, which was just discussed; the second is the 2 α -hydroxyethylidene–TPP intermediate. This is a prochiral center and, as was discussed by Schellenberger, this α -carbanion (“active aldehyde”) will exist when the hydroxy and methyl groups are arranged perpendicular to the plane of the thiazolium ring.⁶⁴ The resonance-

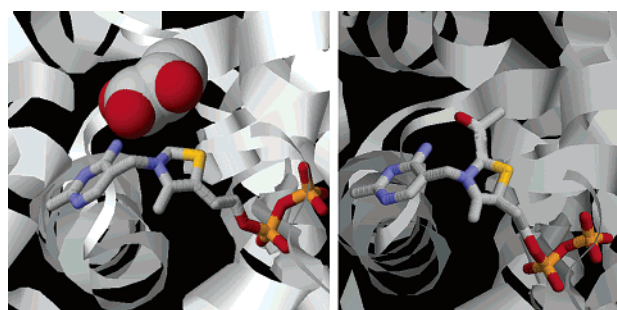


Figure 9. Early intermediates in the PFOR reaction. Left panel: pyruvate–TPP adduct (from PDB code 2PDA), with pyruvate shown as a space-filling model. Right panel: HE–TPP adduct (from PDB code 1KEK). The bound HE group with its long C2–C2(α) bond is shown on the right.

stabilized enamine is considered to be a low-energy state that would inhibit the catalytic mechanism. The transition state corresponding to this intermediate would be a compromise between the enamine (to stabilize the high-energy state) and the α -carbanion (to maximize reactivity). This intermediate is highly nucleophilic, which is helpful for subsequent reaction with an electrophilic second substrate. For PDC, this would be a proton, to produce acetaldehyde, while for transketolase (TK), it would be a second ketose. The negative charge at the α carbon would make this intermediate an excellent electron donor, which is important for PFOR and the related α -ketoacid oxidoreductases.

B. The Fates of HE–TPP: Convergent and Divergent Mechanisms

Depending on the metabolic requirements and contrasting roles of different TPP-dependent enzymes, HE–TPP can participate in diverse reactions (Figure 10). Since this is a highly reducing interme-

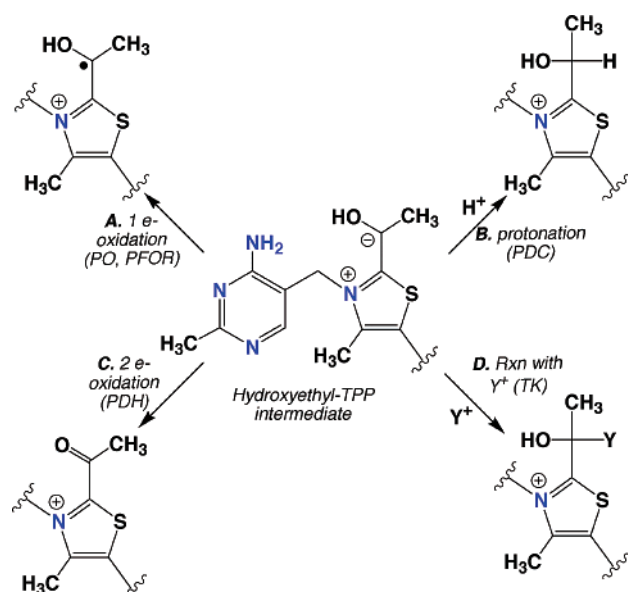


Figure 10. Fates of HE–TPP.

diate, it is poised to undergo one-electron (PFOR, PO) or two-electron (PDH) oxidation, linked to the reduction of flavodoxin/ferredoxin or NAD(P)⁺, respectively. Alternatively, since it is a highly nucleophilic species, it can react with a cationic substrate (TK) or undergo protonation (PDC). It is interesting to speculate about what characteristics of the active site predispose an enzyme to one among these different mechanistic choices. The synchronization of proton transfers in PDC is especially interesting since the enzyme must efficiently deprotonate the thiazolium C2–H to generate the ylide and then protonate the C2 α position, before release of the aldehyde. For PDH, presumably the dihydrolipoamide is in close proximity to attack the HETPP anion and form a tetrahedral thioether intermediate that collapses to generate the acetyldihydrolipoamide–E2(PDH) adduct. Although this reaction reduces a disulfide, it is essentially similar to the nucleophilic reaction performed by TK. How different enzymes choose be-

tween one- and two-electron oxidation is also an interesting question. PFOR and PO contain proximal one-electron acceptors, allowing the formation of two radicals (HE–TPP radical and flavin semiquinone or reduced [4Fe–4S]). For example, the electron transfer to the proximal FeS cluster in PFOR, which is ~ 12 Å from C2, can theoretically occur at a rate of approximately 10^4 s⁻¹.⁶⁵

C. PFOR and Its Radical Mechanism

The overall mechanism of PFOR is shown in Figure 11. Reactions 1 and 2, involving generation of the hydroxyethyl–TPP anion have been discussed above. Reaction 3 involves one-electron oxidation of the anion/enamine intermediate to generate a HE–TPP radical. In the early 1980s, it was recognized that a stable radical intermediate is formed during oxidative decarboxylation of pyruvate by PFOR.^{25,66} How can the radical be detected? The optical absorbance of TPP is very weak compared to the spectra of the FeS clusters. However, like most paramagnetic centers, the HE–TPP radical intermediate can be detected by electron paramagnetic resonance spectroscopy. The X-band Continuous Wave (CW) EPR spectrum of the radical intermediate is centered at $g = 2.00$ and has a peak-to-peak line width of approximately 18 G.^{25,66,67} That this is a substrate-derived radical became clear when the EPR line width, manifested in the hyperfine splittings, was shown to depend on the number of protons at the C-3 position of the α -ketoacid substrate.⁶⁶ Using several 2-oxoacid substrate analogues, it was shown that the radical EPR signal becomes narrower and gradually loses hyperfine structure upon decreasing the number of substrate C-3 bonded protons.²¹ In addition, the EPR line shape of the radical becomes narrower and almost featureless upon substitution of the three protons on carbon 3 of pyruvate with deuterons,⁶⁷ which have a smaller nuclear moment than ¹H (Figure 12). Thus, there are significant interactions between the unpaired spin and the methyl protons of the HE–TPP intermediate, perhaps through a hyperconjugation mechanism. The observation of electron spin coupling between the radical and at least one of the [Fe₄S₄] clusters has indicated that the two paramagnetic species are in close proximity (≤ 10 Å).⁶⁷

D. Electronic Structure of the Radical Intermediate

What is the electronic structure of this radical intermediate? When PFOR was incubated with [3-¹⁴C]- or [2-¹⁴C]-pyruvate, the label remained tightly bound to the enzyme; however, with [1-¹⁴C]-pyruvate, the label was lost, strongly indicating that the substrate-derived radical adduct contains only the hydroxyethyl (or acetyl) portion of pyruvate.⁶⁶ As discussed earlier,⁶⁸ one possibility is that it is a σ -type acetyl radical where little unpaired spin density resides on the TPP cofactor. Another possibility is that the HETPP radical is a π -radical in which there is extensive delocalization of the unpaired electron spin into the thiazolium ring. In Figure 11, it is shown as a π radical with the “dot” on oxygen, but owing to

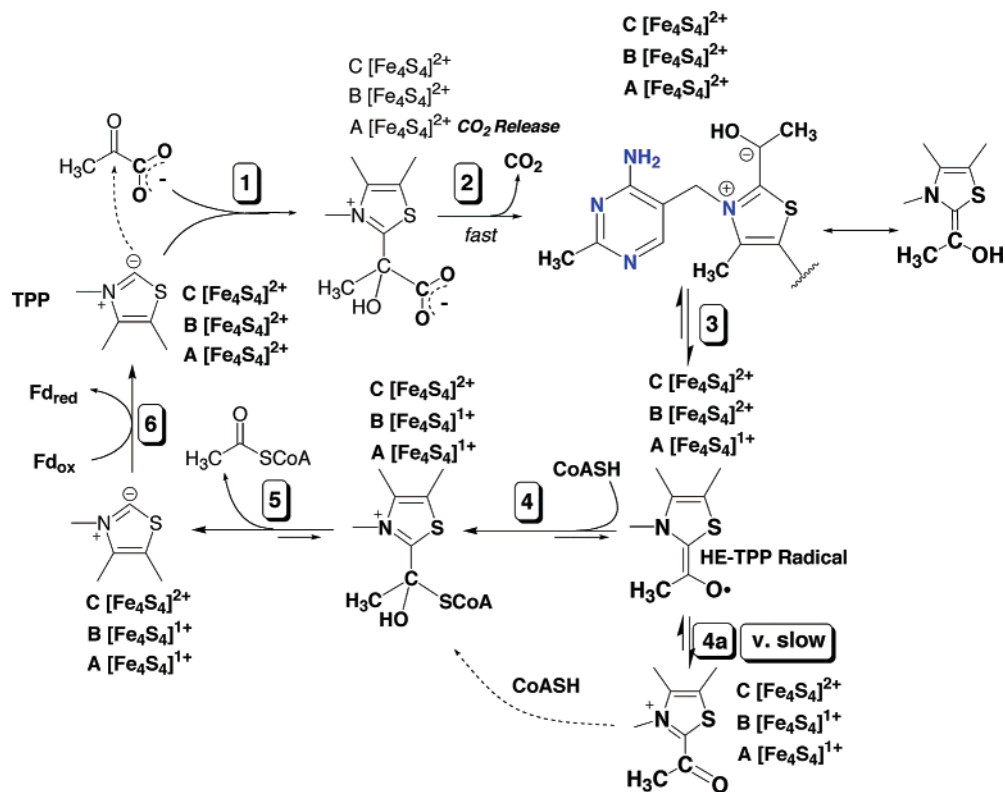


Figure 11. PFOR reaction mechanism, modified from ref 71.

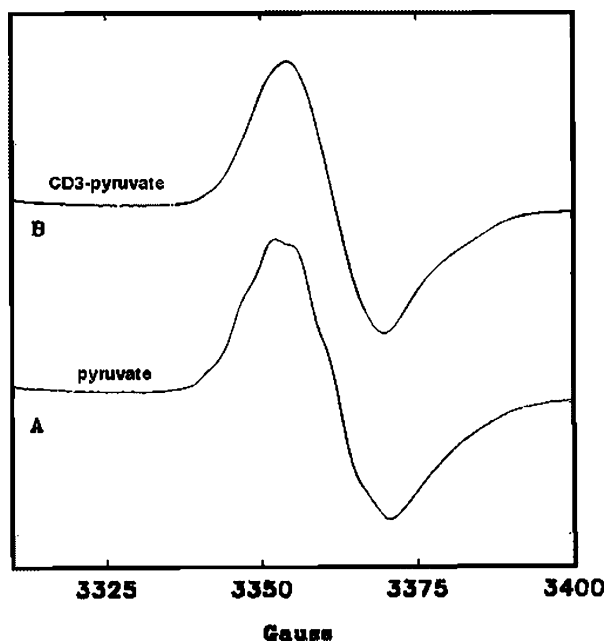


Figure 12. EPR spectrum of PFOR incubated with pyruvate or CD₃-pyruvate. Reprinted from ref 67 with permission.

the aromaticity of the thiazolium, the spin density would be spread over the thiazolium ring. The radical intermediate has been captured at 80% occupancy in the crystal structure of the PFOR from *D. africanus* (Figure 9, above).⁶³ The provocative interpretation of these results is that the thiazolium ring has lost its aromaticity in the radical intermediate to form a σ/n -type radical (Figure 13a). Unusual characteristics of this radical are ketonization of the hydroxy group at C2 α to form an acetyl radical, a long C2–C2 α bond,

sp^3 hybridization at thiazolium atoms N3 and C5, and tautomerization of the C4–C5 double bond to give an exocyclic double bond. Perhaps the most mechanistically significant aspect of this structure is the localization of spin density on the acetyl moiety. This arrangement could facilitate a biradical condensation between the acetyl radical and a CoAS \cdot radical, a possibility discussed below.

Proton and deuterium ENDOR studies of the HE–TPP radical intermediate are consistent with either a σ - (or acetyl-) type radical with little unpaired spin density on the TPP cofactor or a π radical with extensive delocalization of the unpaired electron spin on the thiazolium ring.⁶⁸ These studies revealed two radical species in solution, with slightly different proton hyperfine coupling tensors: $A_{||}^{(1)} = 17.35$ MHz and $A_{\perp}^{(1)} = 11.95$ MHz for the first set of protons and $A_{||}^{(2)} = 19.66$ MHz and $A_{\perp}^{(2)} = 14.66$ MHz, for the other. The slight difference in the coupling tensors reflects slightly different distances between the methyl hydrogens and the carbonyl carbon (1.95 Å for species 1 and 2.11 Å for species 2). For comparison, the molecular geometry average distance between the methyl hydrogens and the carboxyl carbon in H₃CCOOH is 2.150 Å.⁶⁹ Perhaps this reflects an asymmetry between the two subunits in the dimeric unit. The two sets of proton couplings may also reflect two major resonance structures of a π radical intermediate. The π radical can resonate among various structures, some of which are shown in Figure 13b (a more extensive list is provided in Frey's insightful commentary on the Fontecilla–Camps structure.⁷⁰)

In summary, both the σ/n - and π radical structures have been considered as viable options. Further biochemical and biophysical studies are required to

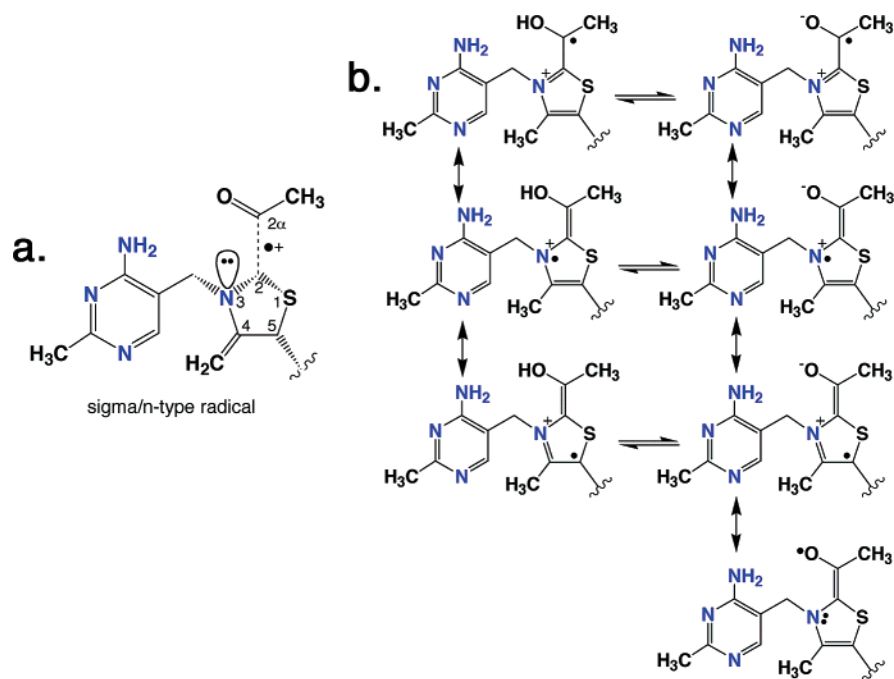


Figure 13. Possible structures of the HE-TPP radical intermediate. (a) Modified from ref 63 and (b) modified from ref 70 with permission from *Science* **2001**, 294. Copyright 2001, American Association for the Advancement of Science.

determine which is an accurate representation. There are several ways one can consider testing the structure-based proposal. One is by EPR, since the π radical is expected to have significant spin density on the thiazolium ring, whereas in the σ/n -type radical, spin density is focused predominantly on C2 α of the acetyl group. Another test, mentioned by Frey in his perspective,⁷⁰ is that the external double bond would allow the hydrogens associated with the methyl substituent at C4 to undergo rapid exchange in D₂O.

E. Reactivity of the HE-TPP Radical Intermediate: Chemical Coupling, Biradicals, and Wires

Is the radical truly a catalytically relevant intermediate in the PFOR reaction, or is it just an interesting artifact? The radical is relatively stable when only pyruvate is added to the enzyme – addition of CoA causes rapid decay.⁶⁶ The decay kinetics, discussed in detail below, strongly indicate the relevance of this radical, an intermediate in the PFOR catalytic mechanism.⁷¹ However, if it is an intermediate, why was it observed in some PFORs and not others, including *Moorella thermoacetica*?^{22,72,73} Two explanations had been offered. One is that the archaeal PFORs use a radical pathway, but bacteria do not.⁴³ The other was that PFORs with an odd number of FeS clusters use a radical pathway while those with an even number do not.⁴⁹ However, it appears likely that the radical had formed and decayed before the sample was frozen for EPR detection. On the basis of rapid freeze-quench EPR and stopped flow studies, this radical intermediate forms and decays significantly faster than the k_{cat} value for the steady-state reaction (5 s⁻¹ at 10 °C for the *M. thermoacetica* enzyme),^{67,71} thus meeting the criteria for a catalytically competent

intermediate in the PFOR reaction mechanism. This rapid radical decay would have prevented its identification in the studies cited above.⁶⁷ Thus, it was argued that all the PFORs are likely to have essentially the same catalytic mechanism, including the intermediacy of a HE-TPP radical, and that this intermediate will be detected in all PFORs when rapid kinetics methods are used to follow the reaction.⁶⁷ PFOR, thus, is a legitimate member of the growing society of enzymes that generate radical intermediates derived from substrates, coenzymes, or amino acid residues,^{74,75} the subject of this volume.

In the absence of CoA, the half-life of the HE-TPP radical intermediate is approximately 2 min; however, in the presence of CoA, the rate of radical decay increases by at least 100 000-fold.⁷¹ Decay of the radical occurs by electron transfer from the HE-TPP radical intermediate to an intramolecular [4Fe-4S] cluster—even in the absence of CoA, decay of the radical intermediate occurs at the same rate as reduction of this cluster.^{67,71} In the presence of CoA, this electron transfer reaction is extremely rapid; even when rapid mixing methods are used, the experiment must be performed below 10 °C to prevent loss of the signal within the dead-time of the instrument (2 ms). The kinetics of radical decay can be followed most quantitatively by measuring the rate of FeS cluster reduction, which results in bleaching of the ~400 nm absorption peak, due to S-to-Fe charge transfer. The same rate is obtained by following decay of the $g = 2.00$ radical EPR signal using freeze-quench EPR techniques; however, with this methodology, one data point is obtained with each experiment. On the other hand, 4000 data points are collected by stopped flow with each mixing experiment. Figure 14 shows the stopped-flow data, which include the chain of electron-transfer events that occur during the catalytic cycle. Radical decay

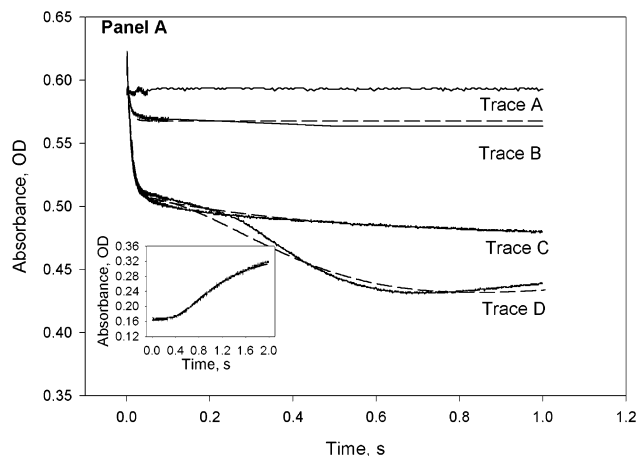


Figure 14. Stopped-flow kinetics of the PFOR reaction with pyruvate and CoA. Reprinted from Figure 6a of Furdai et al.⁷¹

at 10 °C occurs with a half time of 5 ms, indicating that at physiological temperatures for *M. thermoacetica* (above 50 °C), the rate constant for this reaction would be $> 2000 \text{ s}^{-1}$ (half time of 300 μs). The dashed line in Figure 14 is the fit to the overall kinetic mechanism (which is similar to the reaction sequence shown in Figure 11).

The results just described pose some intriguing questions. How does PFOR insulate the reactive centers so that the HE-TPP radical intermediate only reduces the proximal FeS cluster? It is as if the radical and the cluster are in Faraday boxes and a wire connects them only when CoA is present. How does CoA promote the phenomenal acceleration of the electron-transfer rate? Several possible mechanisms have been considered by following the rate of electron transfer from the HE-TPP radical intermediate to its Fe-S cluster acceptor (cluster B) and analyzing the data from transition state and electron transfer theory perspectives.

Rapid electron transfer requires that the donor and acceptor be within $\sim 15 \text{ \AA}$. The relative location of TPP and the FeS clusters is cartooned in Figure 15.

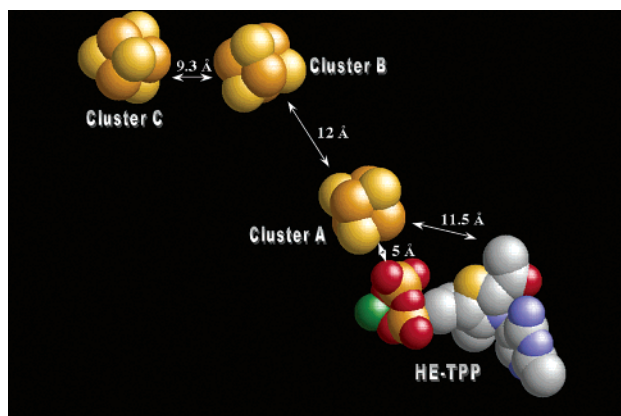


Figure 15. Relative orientation of cofactors in PFOR. From PDB code 2BOP.

The cluster (termed cluster A) that is proximal to TPP undergoes reduction as the radical is formed; thus, decay of the radical occurs either by direct electron transfer from the radical to cluster B, the

medial cluster, or by a “domino-type” process in which cluster A transfers an electron to cluster B and then cluster A is rereduced by the radical. These options are kinetically indistinguishable. Given that the rate enhancement results from some interaction between PFOR and CoA, a structure of this complex would be very useful; however, this has not yet been achieved. We considered that the binding of CoA might be converted into a lowering of the transition state barrier for electron transfer by the so-called “Circe effect”.⁷¹ Although I am not aware of this mechanism being studied for an electron-transfer reaction, it is a factor for several CoA-dependent enzymes.⁷⁶ The binding and kinetic contributions of several CoA analogues were studied, and the most striking results were obtained with desulfo-CoA—its binding energy is only 7 kJ/mol less favorable than that of CoA; yet the decay of the radical intermediate occurs 10^6 -fold slower than in the presence of CoA. This indicates that the thiol group of CoA alone contributes a 40.5 kJ/mol lowering of the free energy of the transition state for electron transfer—clearly, the Circe effect does not play a major role in controlling electron-transfer rates in PFOR.

Marcus analysis of the rate of electron transfer from the HE-TPP radical to the Fe-S cluster indicates that this reaction is “gated”, i.e., the “electron transfer” rate actually reflects the rate of some adiabatic process that is coupled to the redox reaction.⁷¹ What is the gate? Perhaps binding of CoA induces a conformational change that enhances the rate of radical decay, for example, by bringing the redox centers closer together. It was argued that this is not a likely solution to the problem because, although the rate of electron transfer differs by 10^6 -fold between binding of desulfo-CoA and CoA, these analogues should induce similar structural changes.⁷¹

At least three mechanisms of rate enhancement that are consistent with the current kinetic and structural data (Figure 16) have been described.⁷¹ In mechanism A, the kinetic coupling mechanism, the thiol group of CoA performs a nucleophilic attack on the HE-TPP radical to generate a highly reducing anion radical. Assuming that the reorganizational energy and the distance between donor and acceptor are fixed, to achieve the 10^5 -fold increase in electron-transfer rate, a 630 mV difference between the redox potentials of the radical (or anion radical) intermediate and cluster B must be attributed to the thiol of CoA. This does not seem too unreasonable; because of the negative charge density around the radical, this intermediate would have a much higher driving force for electron transfer to cluster B than the HE-TPP radical itself. This mechanism would explain the requirement for the sulfur of CoA, since adduct formation is impossible with desulfo-CoA. In this mechanism, formation of the covalent adduct could be the gate for the electron-transfer reaction. Biomimetic models and theoretical studies are necessary to evaluate the feasibility of this mechanism; I am unaware of any chemical models of such a species or a pair of analogous radicals for comparison.

In mechanism B, the biradical mechanism, a CoA thiyl radical is generated by electron transfer from

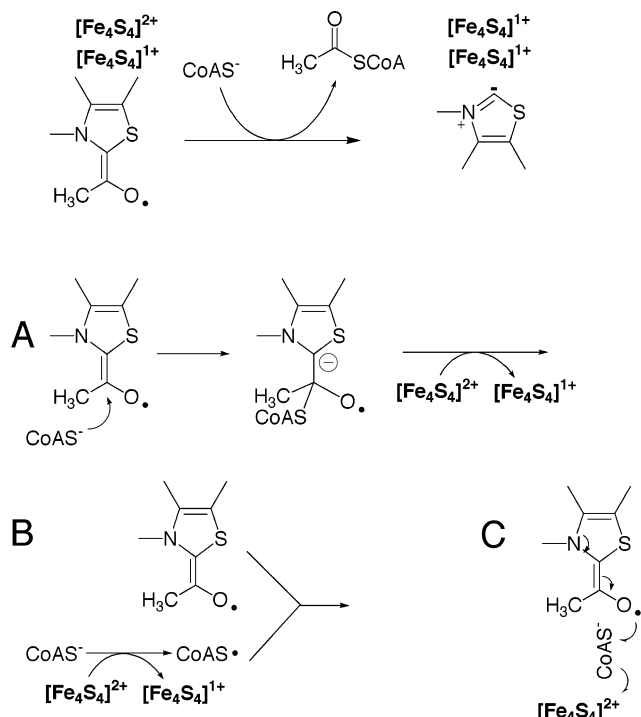


Figure 16. Three mechanisms for enhancing the rate of radical decay. Reprinted from ref 71.

CoA to one of the clusters in PFOR. The resulting thiol radical would combine with the HE-TPP radical. An explanation for the requirement for the sulfur atom of CoA is also explained by this mechanism. Reduction of one Fe-S cluster has been observed when PFOR is reacted with CoA alone, which supports the biradical mechanism.⁶⁷ However, the putative sulfur-based radical has not been observed in such reactions. A CoA thiol radical has been detected in hydrogenosomes from *Tritrichomonas foetus*.⁷⁷ Model studies on the TPP analogs reveal the ease with which HE-TPP radicals recombine in solution.⁷⁸ Mechanism 2 shares some similarities with the PFL reaction mechanism in which a CoA thiol radical is proposed to attack a acetyl-cysteine adduct to generate a cysteine thiol radical and acetyl-CoA.^{79,80} In the crystal structure of the ternary complex of PFL (the nonradical state) with pyruvate and CoA, CoA is in an unusual syn conformation of the N-glycosidic bond leaving the thiol of CoA distant from the carbonyl group with which it will react.⁸⁰ It is proposed that the ribosepentathione group rotates around the glycosidic bond to the favored anti conformation, which would place the CoA sulfur within bonding distance of the carbonyl group of the acetyl-cysteine thioester. This is a clever mechanism of keeping the active thiolate in a waiting position until the acetyl thioester is formed and then swinging it into action by a simple bond rotation that is inexpensive thermodynamically. This mechanism is reminiscent of two adenosylcobalamin-dependent radical enzymes, diol dehydrase⁸¹ and ethanolamine ammonia lyase,⁸² in which the C5' carbon of the 5'-deoxyadenosyl radical swings 7 Å from its "waiting" position as part of adenosylcobalamin to make contact with the reactive group on the substrate.^{83,84} Perhaps a similar rotation could operate in PFOR to promote reaction of a CoA thiol radical with the HE-TPP radical intermediate.

In mechanism C, the wire mechanism, CoA acts as a wire between the HE-TPP radical intermediate and its FeS cluster acceptor. As a wire, CoA would form an effective, though bonded, electron transfer pathway that connects the electron donor, the HE-TPP radical, to the electron acceptor, the FeS cluster. If this mechanism were correct, the electron transfer pathway in the absence of CoA would be inefficient, perhaps involving many through-space jumps or solvent molecules. CoA binding would then induce the formation of a new and favored covalently bonded pathway for electron transfer, which would be more favorable than through solvent or through space.⁸⁵ During the PFOR mechanism, the transition state for thioester formation must involve van der Waals overlap between the CoA thiol group and carbon 1 of the hydroxyethyl moiety. Then the covalent bonds of CoA itself could serve as a ~20 Å long wire that connects the radical intermediate to cluster B. Following the wire analogy, the thiol group of CoA would serve as the prong that connects to the electron source at the socket. Removal of the sulfur atom would create a significant through-space gap that would insulate the donor from acceptor. The wire mechanism would involve a new biological role for CoA. I have some reservations about this mechanism. It appears unlikely that this would be the exclusive mechanism of rate enhancement. If CoA were simply bridging the pathway, I would not expect the resulting electron transfer to be gated, but would be a true electron transfer with an increased coupling. In addition, since most of the covalent electron-transfer pathway should be present in desulfo-CoA, which makes electron transfer 10⁶-fold slower than with CoA, the penalty associated with a single gap between the radical and the methyl carbon (at the beginning of the wire) might not approach such a value. Regardless, further experiments, especially the crystal structure of the PFOR-CoA adduct, are required to test this mechanism.

It is likely that a single mechanism will not account for the electron-transfer rate acceleration and that a combination of the methods described above will be more realistic. Plus, there may be other important effects. Perhaps the binding of CoA induces a change in reorganizational energy as well as in driving force (discussed under the kinetic coupling mechanism, above). Thus, a 0.5 eV decrease in reorganizational energy and a 120 mV stronger driving force could account for the 10⁵-fold increase in the electron-transfer rate. Excluding water from the active site associated with CoA binding would be one way to decrease the reorganizational energy (see below for the discussion on entropy effects). When the rates of electron transfer are studied at different temperatures and the data are treated by the Eyring equation, information about the process that gates electron transfer is obtained.⁷¹ Binding of CoA results in a 32 kJ/mol lowering of the entropic barrier to the electron transfer process, indicating that the rate enhancement is mostly entropic. If the 32 kJ/mol originate from water exclusion, 300 Å² of protein surface shifts from interactions with the solvent to hydrophobic interactions with CoA and/or other

protein residues. This could be explained by release of about 30 molecules of water from the active site when CoA binds to the protein, thus promoting a more compact structure and a lower reorganizational energy, which could enhance the electron-transfer reaction. These issues are discussed in Furdulj and Ragsdale.⁷¹

F. Reaction of Fully Reduced PFOR with Electron Acceptors

Decay of the HE–TPP radical is coupled to acetyl-CoA formation, regeneration of free TPP, and reduction of two FeS clusters (A and B). However, these clusters are buried in the enzyme and cluster C is the direct electron donor to ferredoxin. It appears that another mol of pyruvate reacts to generate a four-electron reduced enzyme before electrons are transferred to ferredoxin.⁷¹ This electron transfer complex involves electrostatic interactions between surface-exposed, negatively charged aspartate and glutamate residues of ferredoxin and lysine residues near cluster C of PFOR.⁸⁶ This scenario is reminiscent of the electron-transfer complex between the *C. pasteurianum* Fd:NADP oxidoreductase and ferredoxin.⁸⁷ Electron transfer is extremely rapid in the PFOR-ferredoxin complex, with a second-order rate constant of $(2-7) \times 10^7 \text{ M}^{-1} \text{ s}^{-1}$, measured by electrochemical methods with the *D. africanus* enzyme.⁸⁶ Nearly the same rate constant is obtained by rapid kinetic studies for the electron transfer from reduced *M. thermoacetica* PFOR to ferredoxin and, interestingly, for electron transfer to oxidized CODH/ACS.³⁰

IV. Perspective and Prospective

PFOR exploits the reducing power of pyruvate to generate low-potential electrons for metabolic energy. In the reverse reaction, it harvests electrons from low-potential donors to fix CO₂ into acetyl-CoA, allowing anaerobic microbes to grow autotrophically. The PFOR structure is known at atomic resolution, including the structure of its substrate-derived radical intermediate. The initial steps of the PFOR reaction mechanism follow the remarkable course of other TPP-dependent enzymes, generating an anionic thiazolium intermediate and then another reactive zwitterion, the hydroxyethyl–TPP intermediate. The elegant studies of Jordan and Huebner to uncover the mechanisms by which transketolase and PDC generate these reactive intermediates guide our thinking about the early steps of the PFOR reaction. It is important to repeat some of these studies with PFOR, for example, determination if PFOR enhances reactivity by lowering the dipole moment at the active site to stabilize the zwitterionic intermediate and measurement of the H/D exchange rates that uncovered the Herculean rate enhancement of deprotonation of the thiazolium. Unlike transketolase or pyruvate decarboxylase, PFOR contains electron sinks (FeS clusters) at appropriate distances that radically alter the course of the reaction. Instead of forming acetaldehyde, an electron is removed from the HE–TPP anionic species (2α -hydroxyethylidene–TPP) to

generate a radical – the “so-called” HE–TPP radical intermediate. On the basis of a high-resolution crystal structure, this radical is proposed to consist of an acetyl radical tenuously bound to a thiazolium ring that has lost its aromaticity. High-resolution magnetic resonance studies should be performed to further explore the structure of the HE–TPP radical and test this provocative hypothesis. The radical intermediate undergoes very slow decay to form a two-electron reduced enzyme. However, the other substrate, CoA, enhances the rate of radical decay by 100 000-fold. The major player in controlling the rate of radical decay, tightly linked to rapid reduction of an FeS cluster, is the sulfur of CoA. Further studies are required to sort out whether CoA controls the electron transfer rate by a chemical coupling mechanism, by forming a thiyl radical to condense with the HE–TPP radical, or by acting as a wire between the radical and an oxidized FeS cluster. Mechanistic studies of appropriate chemical models would greatly enhance our understanding of these reactions steps, as would determination of the crystal structure of the PFOR–CoA complex. The CO₂ that is generated in the PFOR reaction may be transferred directly to CODH/ACS without equilibrating with the solution, a possibility that should be tested. In the spirit of the Introduction, there are many remaining questions. It will require a combination of good biochemistry, biophysics, molecular biology, microbiology, and chemistry to provide the answers.

V. Abbreviations

PFOR	pyruvate ferredoxin oxidoreductase
EPR	electron paramagnetic resonance
ESR	electron spin resonance
ENDOR	electron nuclear double resonance
CoA	Coenzyme A
TPP	thiamine pyrophosphate or thiamine diphosphate
PDC	pyruvate decarboxylase
PO	pyruvate oxidase
PDH	pyruvate dehydrogenase
Fd	ferredoxin
HE–TPP	hydroxyethyl–TPP
TK	transketolase

VI. References

- (1) Lipmann, F. *Annu. Rev. Biochem.* **1984**, *53*, 1.
- (2) Lipmann, F. *Bacteriol. Rev.* **1953**, *17*, 1.
- (3) Banga, I.; Ochoa, S.; Peters, R. A. *Biochem. J.* **1936**, *33*, 1109.
- (4) Banga, I.; Ochoa, S.; Peters, R. *Nature* **1939**, *144*, 74.
- (5) Lohmann, W.; Schuster, G. *Biochem. Z.* **1937**, *294*, 188.
- (6) Reed, L.; DeBusk, B.; Gunsalus, I.; Hornberger, C., Jr. *Science* **1951**, *114*, 93.
- (7) Reed, L. *Adv. Enzymol.* **1957**, *18*, 319.
- (8) Valentine, R. C.; Brill, W.; Wolfe, R. S. *Proc. Nat. Acad. Sci. U.S.A.* **1962**, *48*.
- (9) Mortenson, L. E.; Valentine, R. C.; Carnahan, H. *Biochem. Biophys. Res. Commun.* **1962**, *7*, 448.
- (10) Hughes, N. J.; Chalk, P. A.; Clayton, C. L.; Kelly, D. J. *J. Bacteriol.* **1995**, *177*, 3953.
- (11) Abdel-Hamid, A. M.; Attwood, M. M.; Guest, J. R. *Microbiology* **2001**, *147*, 1483.
- (12) Koike, M.; Koike, K. *Adv. Biophys.* **1976**, *9*, 187.
- (13) Gennis, R. B.; Stewart, V. In *Escherichia coli and Salmonella typhimurium: Cellular And Molecular Biology*, 2nd ed.; Neidhardt, F. C., Ed.; ASM Press: Washington, DC, 1996; Vol. 1.
- (14) Kessler, D.; Knappe, J. In *Escherichia coli and Salmonella typhimurium: Cellular and Molecular Biology*; Neidhardt, F. C., Ed.; ASM Press: Washington, DC, 1996; Vol. 1.
- (15) Wolfe, R. S.; O’Kane, D. *J. Biol. Chem.* **1953**, *205*, 755.

- (16) Uyeda, K.; Rabinowitz, J. C. *J. Biol. Chem.* **1971**, *246*, 3111.
- (17) Raeburn, S.; Rabinowitz, J. C. *Arch. Biochem. Biophys.* **1971**, *146*, 9.
- (18) Raeburn, S.; Rabinowitz, J. C. *Arch. Biochem. Biophys.* **1971**, *146*, 21.
- (19) Uyeda, K.; Rabinowitz, J. C. *J. Biol. Chem.* **1971**, *246*, 3120.
- (20) Horner, D. S.; Hirt, R. P.; Embley, T. M. *Mol. Biol. Evol.* **1999**, *16*, 1280.
- (21) Kerscher, L.; Oesterhelt, D. *Trends Biochem. Sci.* **1982**, *7*, 371.
- (22) Wahl, R. C.; Orme-Johnson, W. H. *J. Biol. Chem.* **1987**, *262*, 10489.
- (23) Kletzin, A.; Adams, M. W. W. *J. Bacteriol.* **1996**, *178*, 248.
- (24) Brostedt, E.; Nordlund, S. *Biochem. J.* **1991**, *279* (Pt 1), 155.
- (25) Cammack, R.; Kerscher, I.; Oesterhelt, D. *FEBS Lett.* **1980**, *118*, 271.
- (26) Peck, H. D., Jr. In *The Sulfate Reducing Bacteria: Contemporary Perspectives*; Odom, J. M., Singleton, R., Jr., Eds.; Springer: Berlin, 1993.
- (27) Postgate, J. R. *The Sulfate Reducing Bacteria*; The Cambridge University Press: Cambridge, 1984.
- (28) Adams, M. W. W.; Kletzin, A. *Adv. Protein Chem.* **1996**, *48*, 101.
- (29) Drake, H. L.; Hu, S.-I.; Wood, H. G. *J. Biol. Chem.* **1981**, *256*, 11137.
- (30) Menon, S.; Ragsdale, S. W. *Biochemistry* **1996**, *35*, 12119.
- (31) Hughes, N. J.; Clayton, C. L.; Chalk, P. A.; Kelly, D. J. *J. Bacteriol.* **1998**, *180*, 1119.
- (32) Ma, K.; Hutchins, A.; Sung, S. J. S.; Adams, M. W. W. *Proc. Natl. Acad. Sci. U.S.A.* **1997**, *94*, 9608.
- (33) Menon, S.; Ragsdale, S. W. *Biochemistry* **1996**, *35*, 15814.
- (34) Muller, M. In *Evolutionary relationships among protozoa*; Coombs, G., Vickerman, K., Sleigh, M., Warren, A., Eds.; Kluwer Academic Publishers: London, 1998.
- (35) Upcroft, J.; Upcroft, P. *Bioessays* **1998**, *20*, 256.
- (36) Hoffman, P. S.; Goodwin, A.; Johnsen, J.; Magee, K.; Veldhuyzen, S. J. O.; Vanzanten, S. *J. Bacteriol.* **1996**, *178*, 4822.
- (37) Meuer, J.; Kuettner, H. C.; Zhang, J. K.; Hedderich, R.; Metcalf, W. W. *Proc. Natl. Acad. Sci. U.S.A.* **2002**, *99*, 5632.
- (38) Simpson, P. G.; Whitman, W. B. In *Methanogenesis: Ecology Physiology, Biochemistry & Genetics*; Ferry, J. G., Ed.; Chapman & Hall: London, 1993.
- (39) Lapado, J.; Whitman, W. B. *Proc. Natl. Acad. Sci. U.S.A.* **1990**, *87*, 5598.
- (40) Bock, A.-K.; Prieger-Kraft, A.; Schönheit, P. *Arch. Microbiol.* **1994**, *161*, 33.
- (41) Tersteegen, A.; Linder, D.; Thauer, R. K.; Hedderich, R. *Eur. J. Biochem.* **1997**, *244*, 862.
- (42) Bock, A. K.; Kunow, J.; Glasemacher, J.; Schönheit, P. *Eur. J. Biochem.* **1996**, *237*, 35.
- (43) Blamey, J. M.; Adams, M. W. W. *Biochim. Biophys. Acta* **1993**, *1161*, 19.
- (44) Rajagopal, B. S.; LeGall, J. *Curr. Microbiol.* **1994**, *28*, 307.
- (45) Bock, A.-K.; Schönheit, P. *J. Bacteriol.* **1995**, *177*, 2002.
- (46) Yoon, K. S.; Hille, R.; Hemann, C.; Tabita, F. R. *J. Biol. Chem.* **1999**, *274*, 29772.
- (47) Zhang, Q.; Iwasaki, T.; Wakagi, T.; Oshima, T. *J. Biochem. Tokyo* **1996**, *120*, 587.
- (48) Chabriere, E.; Charon, M.-H.; Volbeda, A.; Pieulle, L.; Hatchikian, E. C.; Fontecilla-Camps, J.-C. *Nat. Struct. Biol.* **1999**, *6*, 182.
- (49) Pieulle, L.; Guigliarelli, B.; Asso, M.; Dole, F.; Bernadac, A.; Hatchikian, E. C. *Biochim. Biophys. Acta-Protein Struct. Mol. Enzym.* **1995**, *1250*, 49.
- (50) Jordan, F. *FEBS Lett.* **1999**, *457*, 298.
- (51) Breslow, R. *J. Am. Chem. Soc.* **1958**, *80*, 3719.
- (52) Breslow, R. *J. Am. Chem. Soc.* **1957**, *79*, 1762.
- (53) Washabaugh, M. W.; Jencks, W. P. *Biochemistry* **1988**, *27*, 5044.
- (54) Barletta, G.; Huskey, W. P.; Jordan, F. *J. Am. Chem. Soc.* **1992**, *114*, 7607.
- (55) Barletta, G. L.; Huskey, W. P.; Jordan, F. *J. Am. Chem. Soc.* **1997**, *119*, 2356.
- (56) Kern, D.; Kern, G.; Neef, H.; Tittmann, K.; Killenberg-Jabs, M.; Wikner, C.; Schneider, G.; Hubner, G. *Science* **1997**, *275*, 67.
- (57) Jordan, F.; Li, H.; Brown, A. *Biochemistry* **1999**, *38*, 6369.
- (58) Hubner, G.; Tittmann, K.; Killenberg-Jabs, M.; Schaffner, J.; Spinka, M.; Neef, H.; Kern, D.; Kern, G.; Schneider, G.; Wikner, C.; Ghisla, S. *Bba Protein Struct. Mol. Enzym.* **1998**, *1385*, 221.
- (59) Muller, Y. A.; Lindqvist, Y.; Furey, W.; Schulz, G. E.; Jordan, F.; Schneider, G. *Structure* **1993**, *1*, 95.
- (60) Guo, F. S.; Zhang, D. Q.; Kahyaoglu, A.; Farid, R. S.; Jordan, F. *Biochemistry* **1998**, *37*, 13379.
- (61) Huhta, D. W.; Heckenthaler, T.; Alvarez, F. J.; Ermer, J.; Hubner, G.; Schellenberger, A.; Schowen, R. L. *Acta Chem. Scand.* **1992**, *46*, 778.
- (62) Holzer, H.; Beaucamp, K. *Angew. Chem.* **1959**, *45*, 776.
- (63) Chabriere, E.; Vernede, X.; Guigliarelli, B.; Charon, M. H.; Hatchikian, E. C.; Fontecilla-Camps, J. C. *Science* **2001**, *294*, 2559.
- (64) Schellenberger, A. *Bba Protein Struct. Mol. Enzym.* **1998**, *1385*, 177.
- (65) Page, C. C.; Moser, C. C.; Chen, X. X.; Dutton, P. L. *Nature* **1999**, *402*, 47.
- (66) Kerscher, L.; Oesterhelt, D. *Eur. J. Biochem.* **1981**, *116*, 587.
- (67) Menon, S.; Ragsdale, S. W. *Biochemistry* **1997**, *36*, 8484.
- (68) Bouchev, V. F.; Furdui, C. M.; Menon, S.; Muthukumaran, R. B.; Ragsdale, S. W.; McCracken, J. *J. Am. Chem. Soc.* **1999**, *121*, 3724.
- (69) Tabor, W. *J. Chem. Phys.* **1957**, *26*, 974.
- (70) Frey, P. A. *Science* **2001**, *294*, 2489.
- (71) Furdui, C. M.; Ragsdale, S. W. *Biochemistry* **2002**, *41*, 9921.
- (72) Smith, E. T.; Blamey, J. M.; Adams, M. W. W. *Biochemistry* **1994**, *33*, 1008.
- (73) Moulis, J. M.; Davasse, V.; Meyer, J.; Gaillard, J. *FEBS Lett.* **1996**, *380*, 287.
- (74) In *Enzyme-Catalyzed Electron and Radical Transfer*; Holzenburg, A., Scrutton, N., Eds.; Plenum Press: New York, 2000.
- (75) Stubbe, J. *Biochemistry* **1988**, *27*, 3893.
- (76) Jencks, W. P. *Adv. Enzymol.* **1975**, *43*, 218.
- (77) Docampo, R.; Moreno, S.; Mason, R. *J. Biol. Chem.* **1987**, *262*, 12417.
- (78) Barletta, G.; Chung, A. C.; Rios, C. B.; Jordan, F.; Schlegel, J. M. *J. Am. Chem. Soc.* **1990**, *112*, 8144.
- (79) Becker, A.; FritzWolf, K.; Kabsch, W.; Knappe, J.; Schultz, S.; Wagner, A. F. V. *Nat. Struct. Biology* **1999**, *6*, 969.
- (80) Becker, A.; Kabsch, W. *J. Biol. Chem.* **2002**, *277*, 40036.
- (81) Toraya, T. *Chem. Rev.*, in press.
- (82) Reed, G. H. *Chem. Rev.*, in press.
- (83) LoBrutto, R.; Bandarian, V.; Magnusson, O. T.; Chen, X.; Schramm, V. L.; Reed, G. H. *Biochemistry* **2001**, *40*, 9.
- (84) Masuda, J.; Shibata, N.; Morimoto, Y.; Toraya, T.; Yasuoka, N. *Struct. Fold Des.* **2000**, *8*, 775.
- (85) Gray, H. B.; Winkler, J. R. *Annu. Rev. Biochem.* **1996**, *65*, 537.
- (86) Pieulle, L.; Charon, M. H.; Bianco, P.; Bonicel, J.; Petillot, Y.; Hatchikian, E. C. *Eur. J. Biochem.* **1999**, *264*, 500.
- (87) Brereton, P. S.; Maher, M. J.; Tregloan, P. A.; Wedd, A. G. *Biochim. Biophys. Acta* **1999**, *1429*, 307.

CR020423E